Glass fibre composite elements with embedded fibre Bragg grating sensors inspected by thermography techniques

Katarzyna MAJEWSKA[*,1], Magdalena MIELOSZYK[1], Wieslaw OSTACHOWICZ[1,2]

[1] Institute of Fluid Flow Machinery of PASci, Fiszera 14, 80-952 Gdansk, Poland, k.majewska@imp.gda.pl
[2] Warsaw University of Technology, Narbutta 84, 02-524 Warsaw, Poland

Abstract

Composite materials are used extensively in many industry areas, so there is an increasing need of studying their mechanical behaviour in a case of damage occurrence as well as for the non-destructive testing methods for detection of damage initiation and subsequent tracking of its evolution. Due to fibre Bragg grating sensors it is possible to embed an optical fibre into a composite matrix creating a smart element. Its internal structure can be inspected by thermography techniques based on monitoring heat distribution using vibration and/or ultrasonic excitation and/or light impulse in order to evaluate the structural health of the analysed element.

The paper investigates practical aspects of thermography techniques for observation and evaluation of an internal structure of glass fibres reinforced composite laminates with embedded fibre Bragg grating sensors and the discontinuity in a form of a water drop. The experimental investigation is performed on four-layer rectangular sample(s) manufactured during infusion process. In sample between two layers two sensors with different grating length are embedded and between them a drop of water was introduced. The measurements were performed using vibrothermography and impulse thermography techniques. The goal of this paper is to study if it is possible applying thermography techniques to distinguish optical fibres to matrix fibre bundles, to track the arrangement of the optical fibres as well as to find the place where the drop of water was introduced. Additionally the levels of amplitude and frequency of excitation in vibrothermography and time and power of light signal for impulse thermography will be established.

Keywords: structural health monitoring, non-destructive testing, glass fibre reinforced polymer, thermography, fibre Bragg grating sensor, water drop

1. INTRODUCTION

Nowadays, more and more composites are being used in the aerospace, renewable energy, civil and architecture, and other industries, due to their excellent advantages (low cost, light weight, high strength and stiffness to weight ratios) and more longer, greater and more complex composite components are being fabricated (such as wind turbine blade, aircraft parts) which increases manufacturing and maintenance difficulty [2], [5], [7], [9]. Composites reliability guarantee safety of mankind and nature. Nonetheless, structure damage in composite can appear in two ways: by external impacts or by internal failure (delamination, water ingress, dust, finger print, sensors etc.) originated from manufacturing. To overcome the problem is to installed permanently so called structural health monitoring (SHM) systems on/into structure. Due to fibre Bragg grating sensors diameter slightly thicker than a human hair it is possible to embed an optical fibre into a composite matrix creating the SHM system. And it is extremely important to avoid failure while embedding an SHM

systems into composite. There is a lot of non-destructive (NDT) testing techniques to investigate an internal structure of composite. One of the method is infrared (IR) thermography. IR thermography can be divided into two approaches: passive thermography and active thermography. Passive thermography measures thermal variations of a material using an infrared vision device without external thermal sources. Contrary to passive thermography, active thermography requires an external heat sources to stimulate the materials under tests [9]. Despite the fact that thermography has been known for a long time is difficult to found in the literature papers connected to application of thermography to detection of water/ moisture or optical fibre in laminates. Infrared thermography has been proven to be an effective method to detect water ingress in honeycomb parts because water-filled cells have a higher thermal capacity than empty air-filled cells. Transient thermography has become the standard inspection technique for water ingress in honeycomb structures [1].
Guo et al. applied pulsed thermography for water detection in aviation composite honeycomb panels [3]. Vavilov and Nesteruk detected and evaluated water hidden in honeycomb panels of aircraft under exploitation [8]. Chan et al. developed a method to quantify the water ingress by pulsed thermography. As a sample they used 20 mm-thick steel plate and honeycomb sample with a Nomex core and glass fibre skin [1]. Halabe et al. studies on defect detection in GFRP bridge decks focused on air-filled defects as well as fully and partially water-filled defects [4]. Stewart et al. investigated a thermal nondestructive evaluation technique based on thermography that uses optical fibre thermal sensors to detect damage within a laminated graphite epoxy composite specimen. [6].
In the paper Authors applied vibro- and impulse thermography to investigate the discontinuity in a form of a water drop and fibre optic.The paper is organised as follow. Firstly GFRP sample with embedded FBG sensors and drop of water are described. Then the thermography imaging results for the samples are presented. At the end some conclusions and method's limitation is discussed.

2. EXPERIMENTAL INVESTIGATION

The measurements were performed on rectangular GFRP sample. The dimensions of a sample were as follow 70 mm x 200 mm x 1 mm. The sample was made out of four layers of GFRP with two fibre optic with FBG sensors and a drop of water embedded between 1st and 2nd layer counting form the bottom of the sample (Figure 1(b)). The laminates were manufactured using infusion method for bidirectional material (glass SGlass®) and epoxy resin. During preparation process the material was laying on a metal plate covered by PTFE layer allowing easy removing sample. The material plies were covered by additional material layer in a purpose of an equal distribution of the resin during the manufacturing process. Due to this the bottom surface of every sample is smooth while the top one is rough. The physical parameters of a glass material and bare fibre optic are similar. The main difference is that the glass fibres are intertwined making one textile while fibre optics is separated. The dimension of fibre optics is about 0.25 mm and is smaller than the thickness of textile (0.4 mm) used for making one layer of the composite sample. The dimension of a drop of water is no bigger than 5-10 mm cross section and no thicker than one layer of GFRP material.
The internal structure of prepared composite sample was examined using vibrothermography method. The experimental set up is presented in Figure 1(a). Measurements were conducted using signal generator, amplifier, ultrasound exciter, infrared camera Flir SC-5600, universal support frame with pneumatic control and PC computer for infrared camera software operation. Signal form generator after amplification drives the ultrasound exciter. Generated vibrations changed the temperature field of the sample in the places where any discontinuities

(drop of water, fibre optics) were introduced. Temperature changes were registered using infrared camera and PC computer.

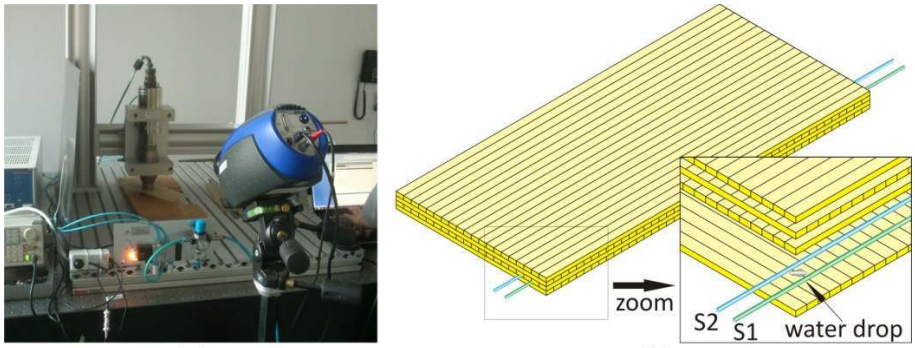

(a) (b)

Figure 1. (a) The set up of vibrothermography with sample, (b) schema of sample with zoom on its internal structure, where S1 and S2 are the fibre optics.

The main purpose of this experimental investigation was to study if it is possible applying thermography techniques to distinguish optical fibres to matrix fibre bundles, to track the arrangement of the optical fibres as well as to find the place where the drop of water was introduced. For this goal the following scenario of measurement was proposed. A sine form of signal from generator after amplification stimulate an ultrasound head to vibrations. The measurements were performed for signal frequency range from 1 kHz to 10 kHz (with step 1 kHz) and a signal peak-to-peak amplitude range varying form 1 Vpp to 20 Vpp (with step 1 Vpp). Vibrations spread in the sample changing local temperature field which was observed due to infrared camera (measurement frequency 100 Hz) and registered in 1500 frame movie due to camera software installed on computer. An example of thermogram for frequency f= 6 kHz and peak-to-peak amplitude ppA= 12 V is shown in Figure 2(a). Additionally the localisation of both fibre optics (S1, S2), drop of water (A, AQUA) as well as pure material (M, MATERIAL) is marked. In every localisations (A, M, S1, S2) three points were chosen for proposed analysis. In Figure 2(b) an average timing-graph is presented – it is clearly visible that all marked areas characterised with different temperature behaviour.

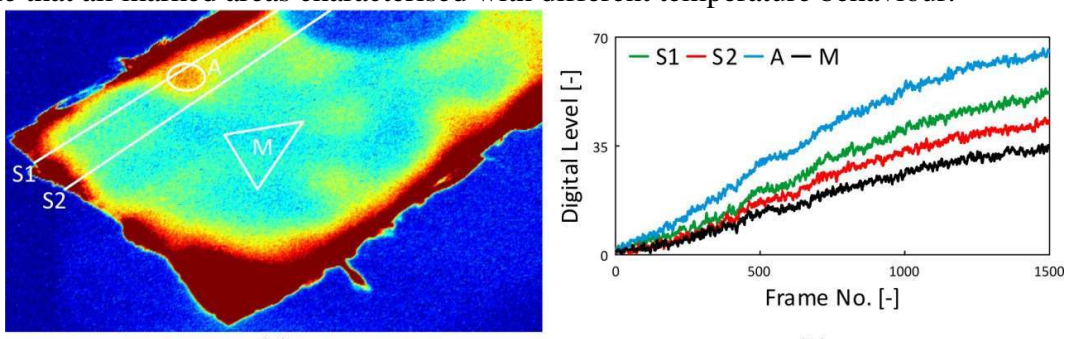

(a) (b)

Figure 2. (a) An example of thermogram (6 kHz and 12V), (b) an average timing-graph for chosen area.

In Figure 3 a map of temperature distribution for frequency range 1–10 kHz and peak-to-peak amplitude range 1-20 V for every area (Figure 3(a) – aqua, Figure 3 (b) material, Figure 3(c) fibre optic S1, and Figure 3(d) fibre optic S2) is presented. It is clearly visible that the highest digital level is achieved for area with drop of water, and the lowest one for pure material. For both optical fibres S1 and S2 distribution of temperature field is almost equal. Inequality in temperature distribution for both fibres is more observable in Figure 4 – compare Figure 4(c)

and Figure 4(d).
This small inequality in the temperature distribution for fibres is connected to the locations of single fibre. The fibre optic S1 is located near the edge of the sample while the fibre optic S2 is more closer to the centre of the sample. In Figure 2(a) is clearly visible the influence on temperature distribution for optic fibre S1 coming from the edge of the sample and from drop of the water. Tracking the Figure 4 allows to see inequality in the temperature distribution for both fibres S1 and S2.

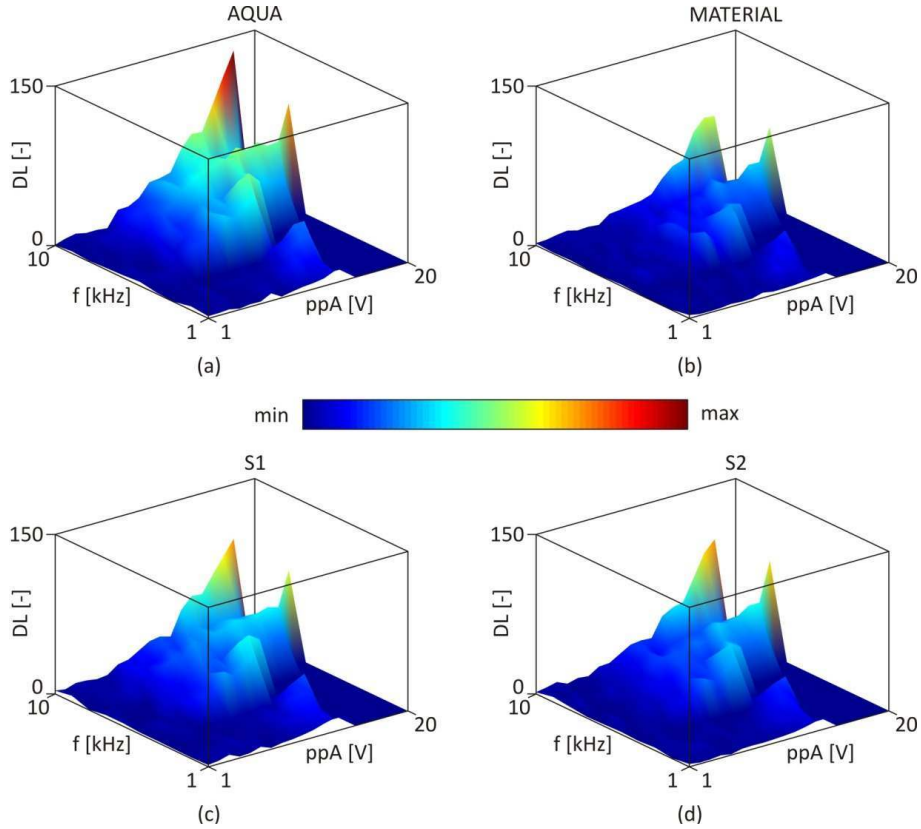

Figure 3. The temperature distribution in function of frequency and peak-to-peak amplitude for selected areas.

The maps in Figure 4 show that in this scenario case a sample is sensitive in peak-to-peak amplitude range from 5 V to 10 V for drop of water A, and both optic fibre S1 and S2 while for material M peak-to-peak amplitude range is 7 V to 10 V. For further analysis of achieved results the frequency f= 6 kHz and peak-to-peak amplitude ppA= 12 V were selected (highlighted as orange straight lines in Figure 4) for all cases (A, M, S1, S2).
In Figure 5 the temperature distribution for frequency 6 kHz in function of peak-to-peak amplitude in range 1 V to 20 V and frame by frame (1500 movie frames in 30 s) is presented. For such a method of presentation of the results (for f= 6 kHz and ppA= 1-14 V) two peak-to-peak amplitudes are dominated one for 13 V and the second one, twice lower for 9 V. The behaviour is stronger for drop of water and pure material than for fibre optics.
Comparing digital levels in all selected areas (Figure 5) it is clearly visible that their values in the area with drop of water (marked as AQUA) are much higher than for the others. It is also easy to see that digital level for pure material is twice lower than for the area with drop of water. Also it is possible to distinguish fibre optic S1 to S2 especially for higher peak-to-peak amplitudes.

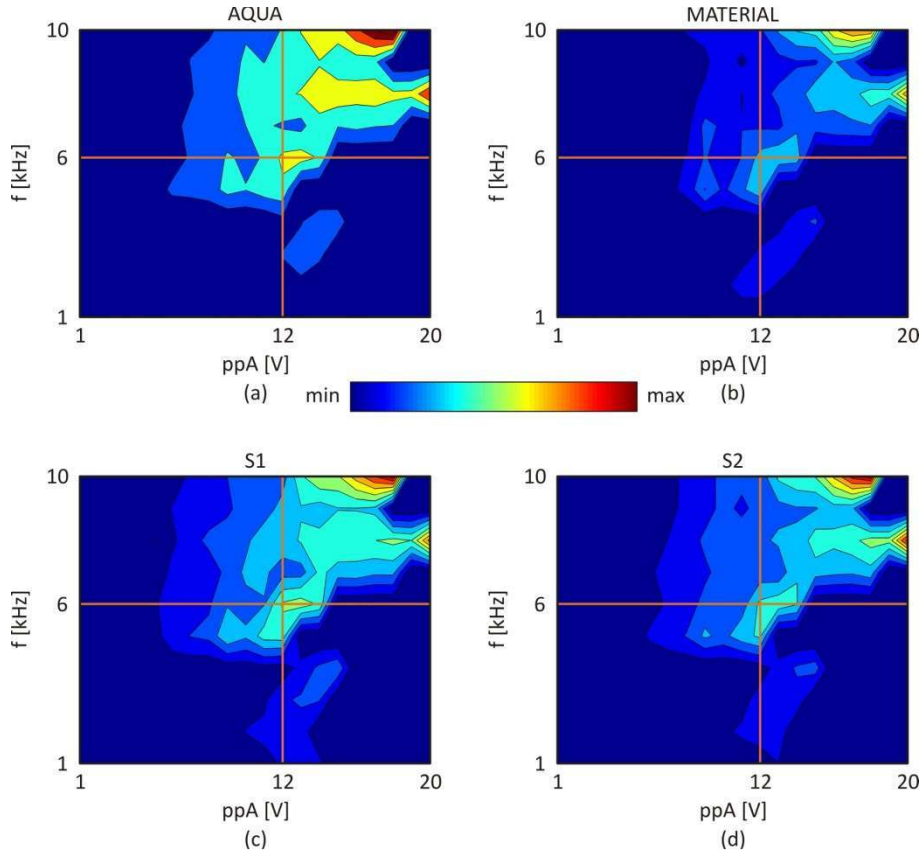

Figure 4. Maps showing relation between frequency and peak-to-peak amplitude for selected areas.

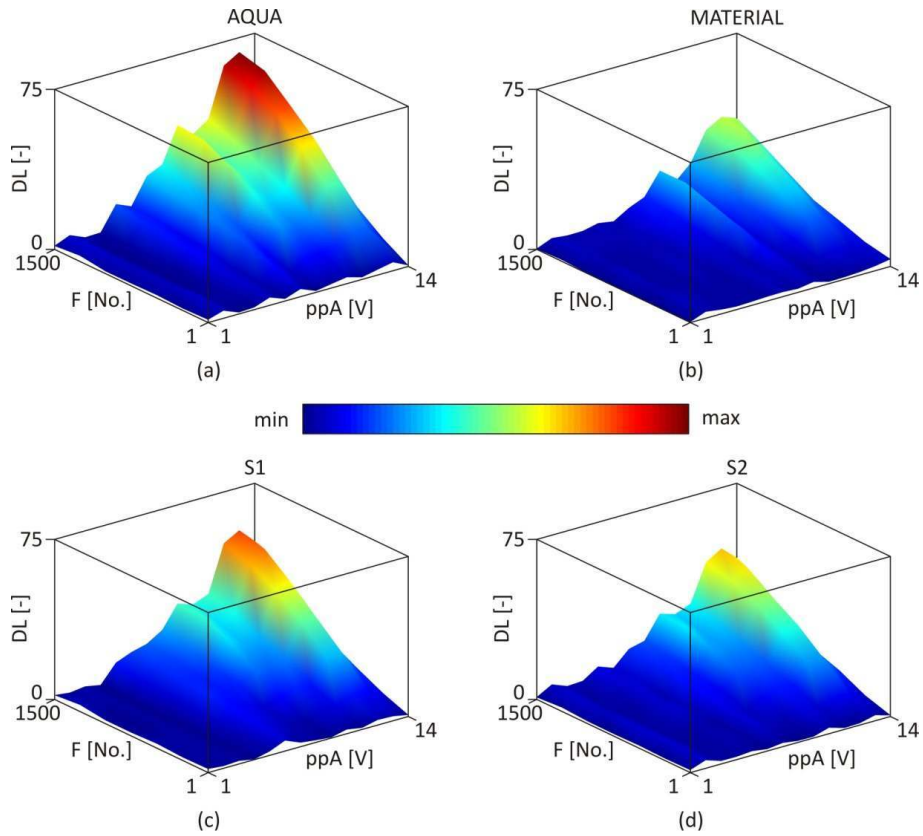

Figure 5. The temperature distribution for 6 kHz in function of peak-to-peak amplitude and frame by frame.

To answer the questions *how drop of water stand out from the material and fibre optics* and *how the fibre optics stands out from the pure material* two simple indicators ($I_{A/i}$ and $I_{j/M}$) were proposed by the following formulas:

$$I_{A/i} = |I_A - I_i|, \text{ where } i = M, S1, S2 \quad (1)$$

$$I_{j/M} = |I_j - I_M|, \text{ where } j = S1, S2 \quad (2)$$

The results for indicators are presented in Figure 6. The (a), (b) and (c) subplots in Figure 6 are showing how significantly a drop of water is visible on the background (pure material, fibre optics) while (d) and (e) subplots showing how fibre optics is visible on pure material.

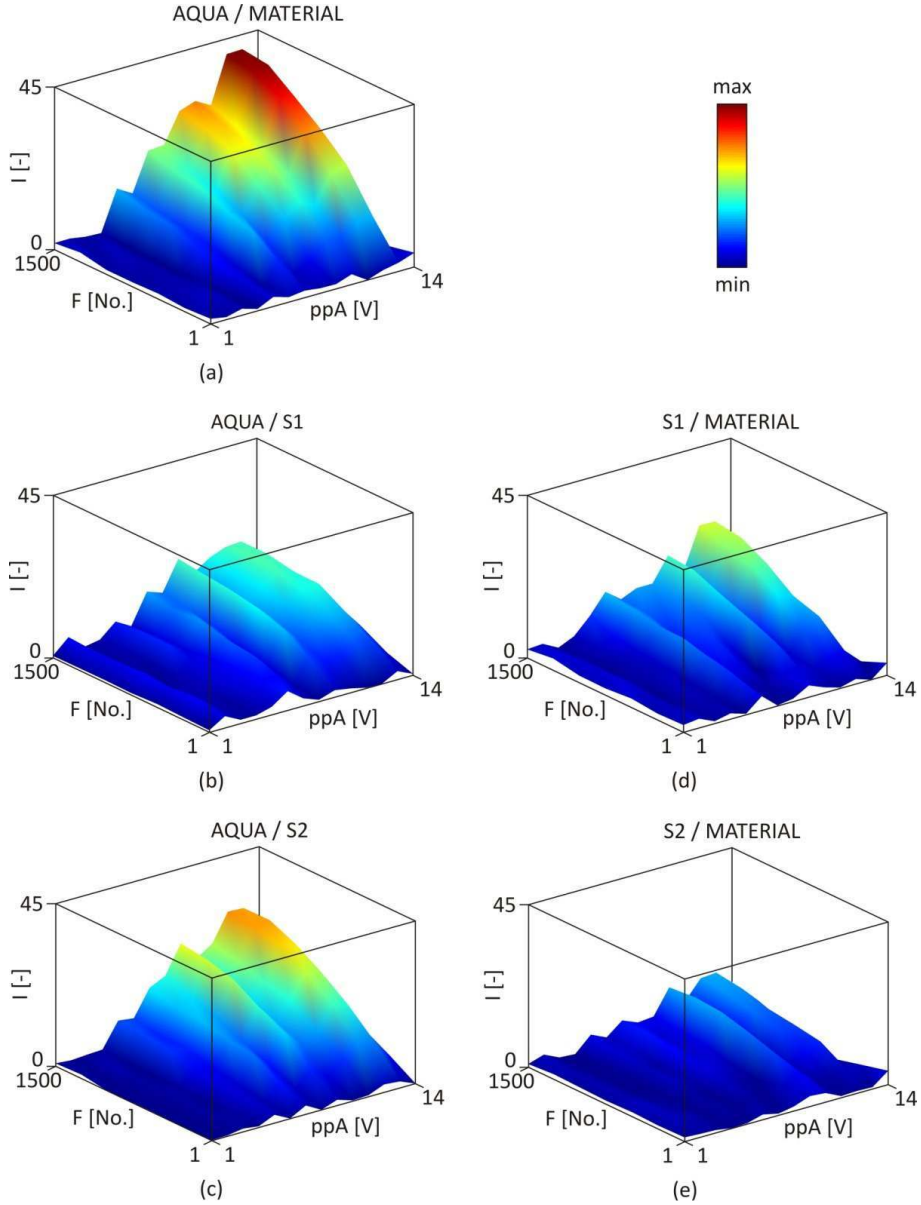

Figure 6. The indicator in function of peak-to-peak amplitude and frame by frame.

The indicators allow to distinguish differences in temperature behaviour for every marked area for lower values of peak-to-peak amplitudes than it was in pure cases (Figure 5).
In Figure 7 the temperature distribution (in digital level values) for peak-to-peak amplitude

12 V in function of frequency in range 1 kHz to 10 kHz and frame by frame (1500 frames/ 30 s) is presented.

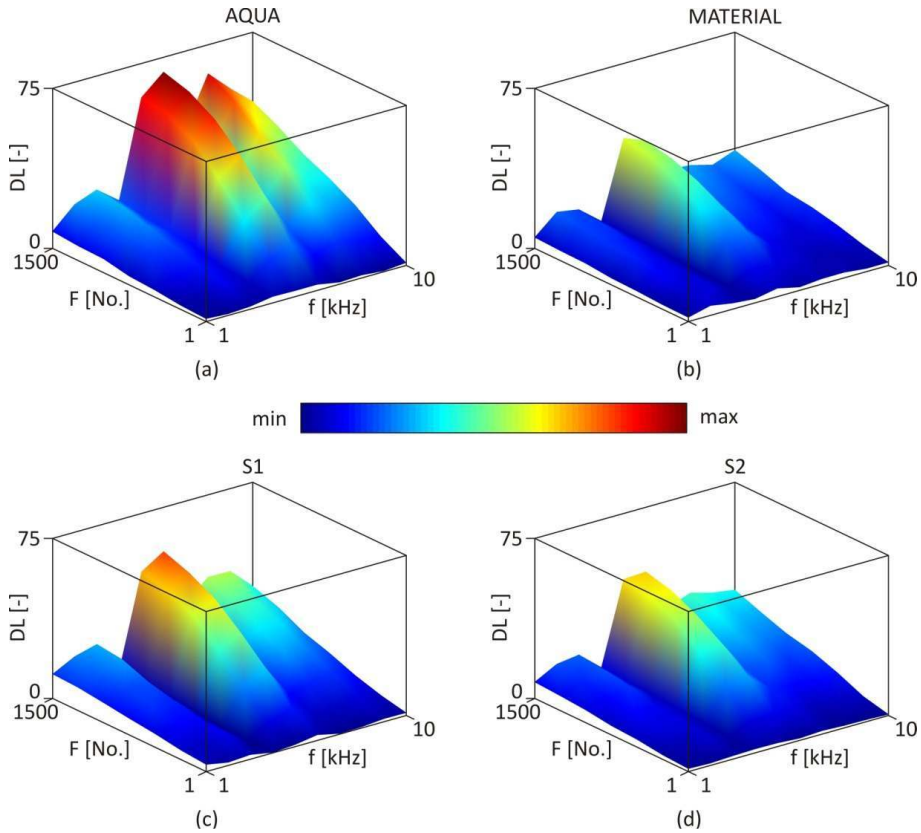

Figure 7. The temperature distribution for 12 V in function of frequency and frame by frame.

For such a method of presentation of the results (for f= 1-10 kHz and ppA= 12 V) three frequencies are dominated (5 kHz, 6 kHz and 8 kHz). For drop of water the significant frequencies are: 6 kHz and 8 kHz, while for material and fibre optics are 5 kHz and 6 KHz. The behaviour is twice stronger for drop of water than for pure material or fibre optics. Note that for all selected areas the dominated frequency is 6 kHz.

Also in this case to answer the questions *how drop of water stand out from the material and fibre optics* and *how the fibre optics stands out from the pure material* indicators ($I_{A/i}$ and $I_{j/M}$) (formula (1) and formula (2)) were used and analised. The results for indicators are presented in Figure 8. The (a), (b) and (c) subplots in Figure 8 are showing how significantly a drop of water is visible on the background (pure material, fibre optics) while (d) and (e) subplots showing how fibre optics is visible on pure material. The indicators allow to distinguish differences in temperature behaviour for every marked area for lower values of frequency than it was in pure cases (Figure 7).

Comparing indicator distribution in a function of peak-to-peak amplitude (Figure 6) or frequency (Figure 8) it seems that proposed methodology is more sensitive to peak-to-peak amplitude. Sensitivity here means that for established frequency and variety of peak-to-peak amplitude the value of indicators differ for each peak-to-peak amplitude change. There is no such a indicators sensitivity observed for frequency changes. For frequency changes the indicators changes are much smoother.

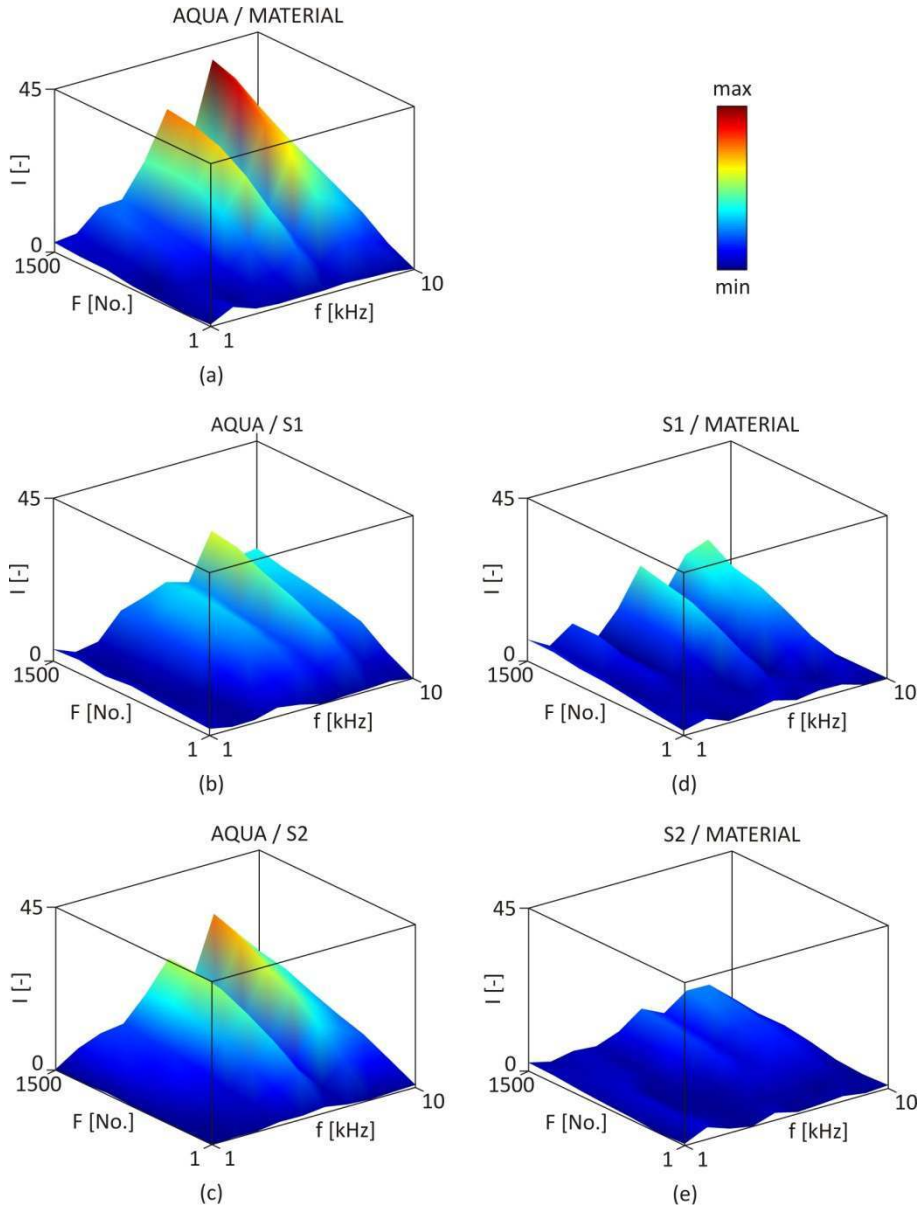

Figure 8. The indicator in function of frequency and frame by frame.

In Figure 9 the map of indicators values in function of frequency and peak-to-peak amplitude is presented. It is clearly visible that the proposed indicators are sensitive for any change of frequency or peak-to-peak amplitude. It is also easy to observe that indicators values for drop of water is much higher than for fibre optics. For both proposed indicators dominated indicator value revealed for f= 10 kHz and ppA= 18 V, but for aqua indicator value $I_{A/M}$ is equal almost 70 while for indicator value $I_{S1/M}$ is 25.

For the same sample the impulse thermography trials were made. In the case the sample was hanged on special frame and reflected with two halogen lamps (150 W each). The response from the sample was observed via infrared camera standing on the same side as lamps. In Figure 10(b) a selected thermogram of the sample with fibre optics and drop of water under impulse thermography is presented. On this thermogram it is clearly visible the drop of water area (black circle) and both of fibre optic (marked as S1 and S2). Also on the left hand side of Figure 10(b) the light green/yellow colour reveals thinner area of the sample. This effect was not observed for vibrothermograpy.

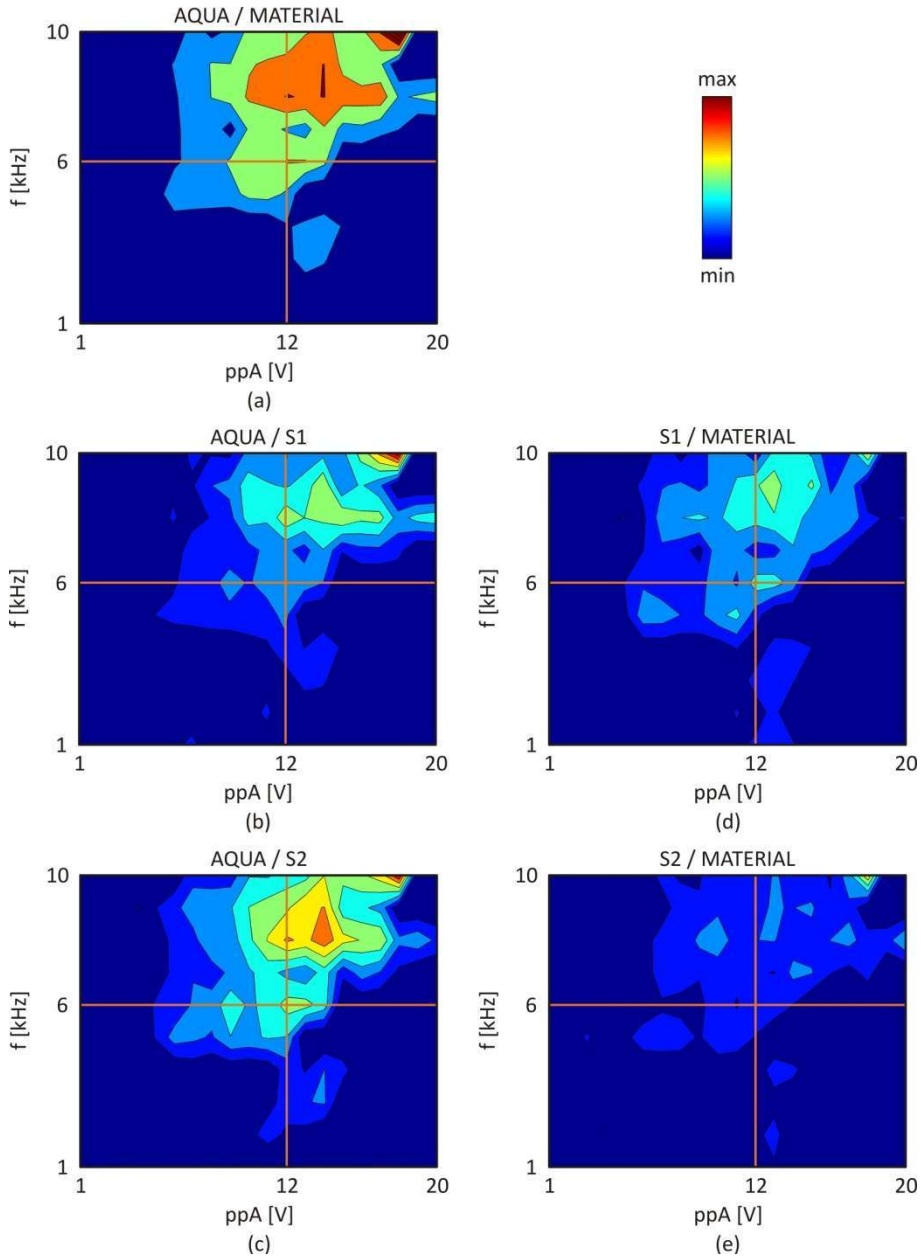

Figure 9. Maps showing relation between frequency and peak-to-peak amplitude for proposed indicators.

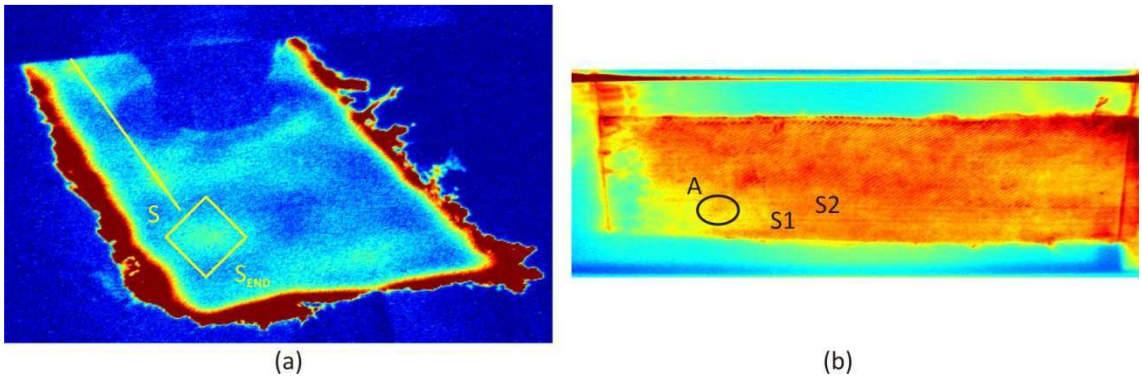

Figure 10. Thermogram of (a) a sample with broken fibre optic (vibrothermography) (b) a sample with fibre optics and drop of water (impulse thermography).

In Figure 10(a) the possibility of finding a place where the fibre optic broke is shown. The thermogram of different sample (made as it was mentioned before – but only with fibre optics) presents the fibre optic track marked as S and additionally the place where the fibre optic broke (yellow rhombus with S_{end}). This thermogram was made for frequency 6 kHz and peak-to-peak-amplitude 12 V.

CONCLUSIONS

The paper investigates practical aspects of thermography techniques for observation and evaluation of an internal structure of GFRP with embedded fibre optics and the discontinuity in a form of a water drop. The main conclusion is that it is possible to find a fibre optic or to localise the place of broken fibre optic as well as to localise place of drop of water. The proposed simple indicators show the sensitivity of changes the peak-to-peak amplitudes and frequencies for selected area. Notice that the single fibre optic is 7% while drop of water is less than 0.5% of the volume fraction of the sample. Two different approaches (vibro- and impulse thermography) for the same sample reveal that for same defects vibrothermograpy is better and for some impulse one – complex combination of different thermography approaches is needed to have complex response about sample structural condition.

ACKNOWLEDGEMENTS

This research was supported by the project entitled: Non-invasive Methods for Assessment of Physicochemical and Mechanical Degradation granted by National Centre for Research and Development in Poland - Project No. PBS1/B6/8/2012.

REFERENCES

[1] Chen D., Zeng Z., Zhang C., Jin X., Zhang Z. Quantitative study of water ingress in pulsed thermography. *Insight* **55(5)**, 257-263, 2013.

[2] Fernandes H., Zhang H., Maldague X. An active infrared thermography method for fiber orientation assessment of fiber-reinforced composite materials. *Infrared Physics & Technology* **72**, 286–292, 2015.

[3] Guo X., Zhang F. Study on pulsed thermography to detect water ingress in composite honeycomb panels. Proc. of 11th QIRT International Conference, Naples, Italy, 2012.

[4] Halabe U.B., Roy M., Klinkhachorn P., GangaRao H.V.S. Detection of air and water-filled subsurface defects in GFRP composite bridge decks using infrared thermography. Proc. of AIP Conference, Brunswick, ME, USA, 2005.

[5] Lizaranzu M., Lario A., Chiminelli A., Amenabar I. Non-destructive testing of composite materials by means of active thermography-based tools. *Infrared Physics & Technology* **71,** 113–120, 2015.

[6] Stewart A., Carman G., Richards L. Thermography technique for graphite/epoxy composite structures utilizing embedded thermal fiber optic sensors. Proc of SPIE Vol. 5056, 2003.

[7] Usamentiaga R., Venegas P., Guerediaga J., Vega L., López I. Automatic detection of impact damage in carbon fiber composites using active thermography. *Infrared Physics & Technology* **58**, 36–46, 2013.

[8] Vavilov V., Nesteruk D. Evaluating water content in aviation honeycomb panels by transient IR thermography. Proc. of SPIE Vol. 5782, 2005.

[9] Yang R., He Y. Optically and non-optically excited thermography for composites: A review. *Infrared Physics & Technology* **75**, 26–50, 2016.